Structural Studies and Computer Simulation of the Inclusion of Aromatic Hydrocarbons in a Zinc 2,6-Naphthalene Dicarboxylate Framework Compound

R. Nandini Devi,[†] Mark Edgar,[†] Jorge Gonzalez,[†] Alexandra M. Z. Slawin,[†] David P. Tunstall,[‡] Paramjit Grewal,[§] Paul A. Cox,*[,§] and Paul A. Wright*[,†]

School of Chemistry, University of St. Andrews, Purdie Building, North Haugh, St Andrews, Fife, KY16 9ST, U.K., School of Physics and Astronomy, University of St. Andrews, North Haugh, St Andrews, Fife KY16 9SS, U.K., and Centre for Molecular Design, University of Portsmouth, King Henry Building, Portsmouth PO1 2DY, U.K.

Received: May 30, 2003; In Final Form: October 24, 2003

We have examined the structural response of a zinc 2,6-naphthalene dicarboxylate framework solid, isostructural with MOF-105, to the inclusion during crystallization of dimethylformamide, benzene, toluene, and *p*-xylene. These compounds, which are made up of a stacked arrangement of four-connected layers, crystallize in the space group $P2_1/c$ with $[Zn_2(ndc)_2(DMF)_2]\cdot 1.6DMF$ (**1**), $a = 8.075(1)$ Å, $b = 16.891(2)$ Å, $c = 12.673(2)$ Å, $\beta = 92.90(1)°$, $[Zn_2(ndc)_2(DMF)_2]\cdot C_6H_6$ (**2**) $a = 8.340(2)$ Å, $b = 15.660(4)$ Å, $c = 13.008(4)$ Å, $\beta = 91.340(5)°$, $[Zn_2(ndc)_2(DMF)_2]\cdot C_7H_8$ (**3**), $a = 8.183(2)$ Å, $b = 16.245(3)$ Å, $c = 12.920(3)$ Å, $\beta = 91.976(4)°$, and $[Zn_2(ndc)_2(DMF)_2]\cdot C_8H_{10}$ (**4**), $a = 7.973(2)$ Å, $b = 16.946(3)$ Å, $c = 12.922(3)$ Å, $\beta = 92.798(4)°$. The structure is found to include *p*-xylene with high selectivity from mixtures of xylene isomers. In the presence of only *o*- or *m*-xylene as an additive, the structure does not crystallize. The mobility of fully deuterated benzene and toluene within compounds **2** and **3** over the temperature ranges 123−294 and 173−294 K, respectively, has been measured by ^2H NMR using the quadrupole echo technique. Benzene is found to execute rapid hopping around its C_6 axis over the entire temperature range studied with an activation energy of 6(1) kJ mol^{-1}. The only motion of the toluene is rapid rotation of the $-CD_3$ group. Computational modeling of the structures successfully reproduces the crystal structures and the changes in unit cell parameters and indicates that the binding energies of *m*-xylene within the structure are less favorable than those for *p*-xylene, predominantly as a result of the distortion of the framework required to accommodate the *m*-xylene. These lower binding energies explain the high selectivity for the uptake of *p*-xylene during crystallization.

I. Introduction

The ability of zinc to form a wide range of coordination polymers, particularly with di- and tricarboxylates, has been one of the most successful areas of the developing field of metal organic frameworks.[1−5] Two- and three-dimensionally connected lattice compounds and frameworks have been crystallized from organic solvents and from aqueous media. Some of these frameworks are stable to the removal of solvent included during crystallization, leaving porous solids, whereas others recrystallize upon ligand removal or exchange.[6] The solids exhibit novel adsorption properties, often possessing very high specific surface areas, and are therefore of interest in the storage of gases such as hydrogen and methane.[5] Related zinc carboxylate solids have also been demonstrated to exhibit properties such as the characteristic blue fluorescence of zinc compounds.[7]

Our work[6] on a family of zinc 1,4-benzene dicarboxylates, crystallized at room temperature from dimethylformamide solution from the reaction of a zinc salt with a deprotonated carboxylic acid, according to the method of Yaghi,[2] demonstrated the high reactivity of some of these layered materials in which solvent loss and ligand exchange resulted in reconstructive transformations and ultimately recrystallization. The DMF molecules included upon crystallization are hydrogen-bonded to the zinc 1,4-benzene dicarboxylate lattice and could not be removed or exchanged by other molecules, such as methanol, without major structural change. One of the most attractive features of metal−organic frameworks is that the size of their cavities can be controlled by changing the length of the organic spacers. We therefore chose to investigate the behavior of 2,6-naphthalene dicarboxylate in preparations similar to the previous work with zinc 1,4-benzene dicarboxylates, because the intraframework void spaces would be expected to be larger and should therefore permit the inclusion of uncoordinated molecules into the pore space.

Here we report the results of crystallization of zinc 2,6-naphthalene dicarboxylate ($Zn_2C_{10}H_6(CO_2)_2\cdot(OCHN(CH_3)_2)_2\cdot R$, R = DMF, benzene, toluene, and *p*-xylene) from DMF solution in the presence (and absence) of aromatic hydrocarbons. The crystallizing phases possess the zinc 2,6-naphthalene dicarboxylate two-dimensional framework including chlorobenzene that has been reported previously as MOF-105.[8] Our work indicates that a range of aromatic hydrocarbons can be included into the structures as they crystallize and that the included species influence the thermal stability of the inclusion compound. We discuss the mobility of these included molecules as measured by ^2H NMR spectroscopy, a technique that yields information on the mode of motion of deuterated species within zeolitic and other solids.[9−13] In addition, we find that the

[†] School of Chemistry, University of St. Andrews.
[‡] School of Physics and Astronomy, University of St. Andrews.
[§] University of Portsmouth.

10.1021/jp0306949 CCC: $27.50
Published on Web 12/13/2003

TABLE 1: Crystallographic Data and Data Collection Parameters for Compounds 2, 3, and 4

empirical formula	$Zn_2C_{30}H_{26}N_2O_{10}\cdot C_6H_6$	$Zn_2C_{30}H_{26}N_2O_{10}\cdot C_7H_8$	$Zn_2C_{30}H_{26}N_2O_{10}\cdot C_8H_{10}$
fw	783.38	797.40	811.43
crystal size	0.1 × 0.1 × 0.03	0.1 × 0.1 × 0.02	0.1 × 0.1 × 0.015
crystal system	monoclinic	monoclinic	monoclinic
space group	$P2_1/c$	$P2_1/c$	$P2_1/c$
a, Å	8.340(2)	8.1834(16)	7.9731(16)
b, Å	15.660(4)	16.254(3)	16.946(3)
c, Å	13.008(4)	12.920(3)	12.922(3)
α, deg	90	90	90
β, deg	91.340(5)	91.976(4)	92.798(4)
γ, deg	90	90	90
V, Å^3	1698.5(8)	1717.6(6)	1743.8(6)
Z	2	2	2
d_{calcd}, mg/m^3	1.532	1.542	1.545
μ, mm^{-1}	1.474	1.459	1.439
F(000)	804	820	836
reflns collected	8271	7148	5999
independent reflns	2401	2404	2417
data/restraints/params	2401/0/229	2404/5/236	2417/0/239
GOF on F^2	0.925	0.922	0.963
R_1 [$>2\sigma(I)$]	0.0526	0.0357	0.0430
wR_2	0.1065	0.0690	0.0916

inclusion process is highly selective for *p*-xylene compared to *o*- or *m*-xylene.

These experimental observations are investigated by computational simulation using density functional theory. Density functional theory (DFT) is a first principles quantum mechanical approach that relies on calculating the electron density of the system via the Kohn−Sham equations.[14] The electron density can be used to determine the ground-state energy and thereby to optimize the geometry of the structure, as well as calculate other properties such as the charge distribution. Although many framework solids of this type have recently been discovered, there has been relatively little work on the computer simulation of their structure and properties. Here we find that details of the structures can be simulated with encouraging accuracy using these methods. The calculations also indicate the origin of the selective uptake of *p*-xylene during crystallization.

II. Experimental Methodology

Synthesis. Zinc 2,6-naphthalene dicarboxylates were crystallized at room temperature from a solution of zinc nitrate and 2,6-naphthalene dicarboxylic acid in dimethylformamide by the slow diffusion of triethylamine to facilitate the deprotonation of the acid. A series of experiments was carried out with the addition of benzene, toluene, and *ortho*-, *meta*-, and *para*-xylene (*o*-, *m*-, and *p*-xylene) to the reaction mixture to investigate their effects on the crystallization. In a typical experiment, triethylamine was allowed to diffuse slowly over a solution of $Zn(NO_3)_2\cdot 6H_2O$ (0.04 g, 0.13 mmol) and 2,6-naphthalene dicarboxylic acid (0.045 g, 0.21 mmol) in dimethylformamide, DMF (20 mL), or mixtures of DMF with aromatic hydrocarbons (15 mL/10 mL). Solid crystalline material was collected after 2 days, filtered, and dried in air. To enable studies of the mobility of the included species, crystallizations were also performed in the presence of perdeuterated benzene and toluene.

Elemental analysis of the crystalline products was performed on a Carlo Erba 1108 instrument. Thermogravimetric analyses, both alone and coupled with mass spectroscopic analysis of the products of heating, were performed using a heating rate of 10 °C/min.

X-ray Crystallography. X-ray powder diffraction of the products was performed in transmission mode on a STOE Stadi/p diffractometer using monochromated Cu $K\alpha_1$ X-radiation (λ = 1.540 56 Å). Where possible, single crystals were selected for crystal structure solution, and the crystals were examined at 125 K on a Bruker SMART X-ray system employing graphite monochromated Mo Kα radiation (λ = 0.710 73 Å) equipped with a CCD detector. The structures were solved by direct methods and refined by full matrix least-squares on F^2 using the SHELXL-97 program.[15] Crystal data are summarized in Table 1. Crystallographic data (excluding structure factors) for the structures reported in this paper have been deposited as supplementary information (CCDC reference numbers 220250−220252).

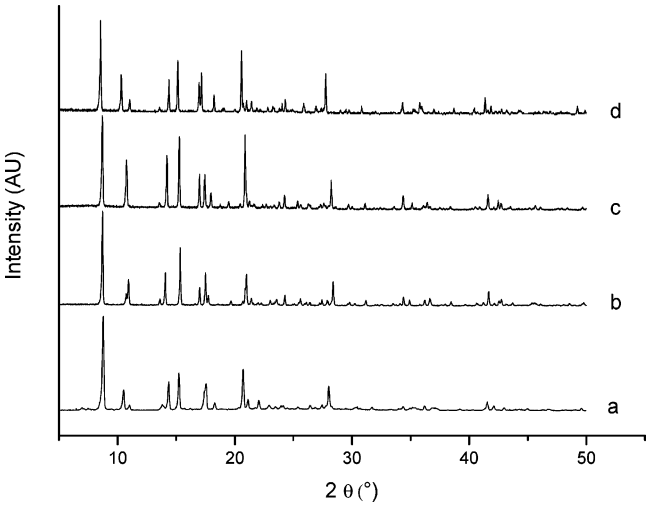

Figure 1. X-ray powder diffraction patterns of (a) $[Zn_2(ndc)_2(DMF)_2]\cdot$1.6DMF (**1**), (b) $[Zn_2(ndc)_2(DMF)_2]\cdot C_6H_6$ (**2**), (c) $[Zn_2(ndc)_2(DMF)_2]\cdot C_7H_8$ (**3**), and (d) $[Zn_2(ndc)_2(DMF)_2]\cdot C_8H_{10}$ (**4**).

Solid-State NMR. ^{13}C CPMAS NMR was performed on a Varian Infinityplus spectrometer operating at 500.155 MHz for ^1H and 125.762 MHz for ^{13}C with a 4 mm Chemagnetics T_3 probe. Fully relaxed ^2H static wide-line spectra were obtained at 76.775 MHz on the same instrument. A quadrupole echo technique was used to record all ^2H spectra in two sets of experiments with the delay between pulses set at 20 and 200 μs. The 90° pulse was set at 3.00 μs, and the spectral width was 2000 kHz with dwell time 0.5 μs. The ^2H spectra were simulated using the web-based program Weblab.[16] Variable temperature ^2H NMR was carried out for compounds **2** and **3** for ranges of 294 K down to 123 and 173 K, respectively. Spin−lattice relaxation measurements were made for compound **2**

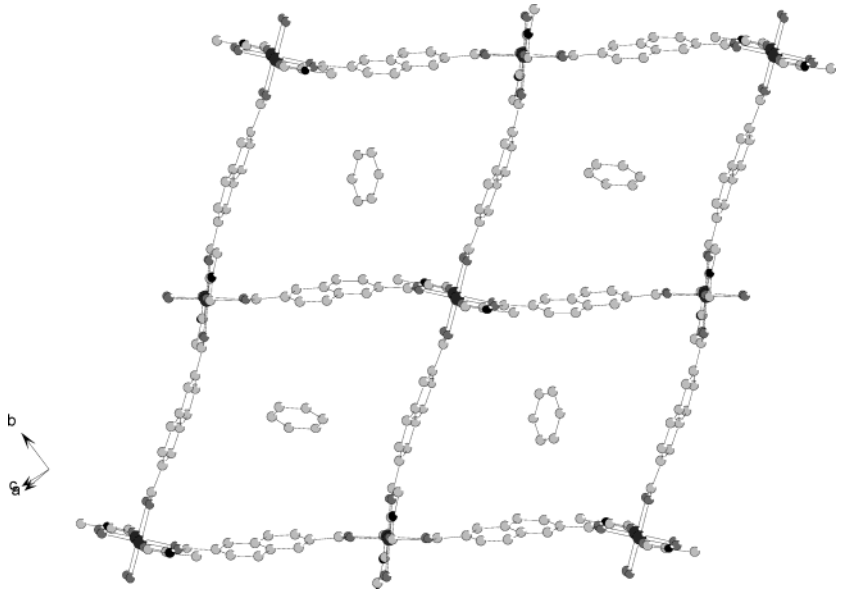

Figure 2. View, in projection, onto an individual layer of the zinc 2,6-naphthalene dicarboxylate MOF-105 structure showing the dimeric units of ZnO_5 square pyramids linked by 2,6-naphthalene dicarboxylate spacers to give a 4-connected lattice with large spaces. Solvent molecules are not shown, and hydrogen atoms are omitted for clarity. Light gray represents C; black represents N; large, dark gray represents Zn; small, dark gray represents O.

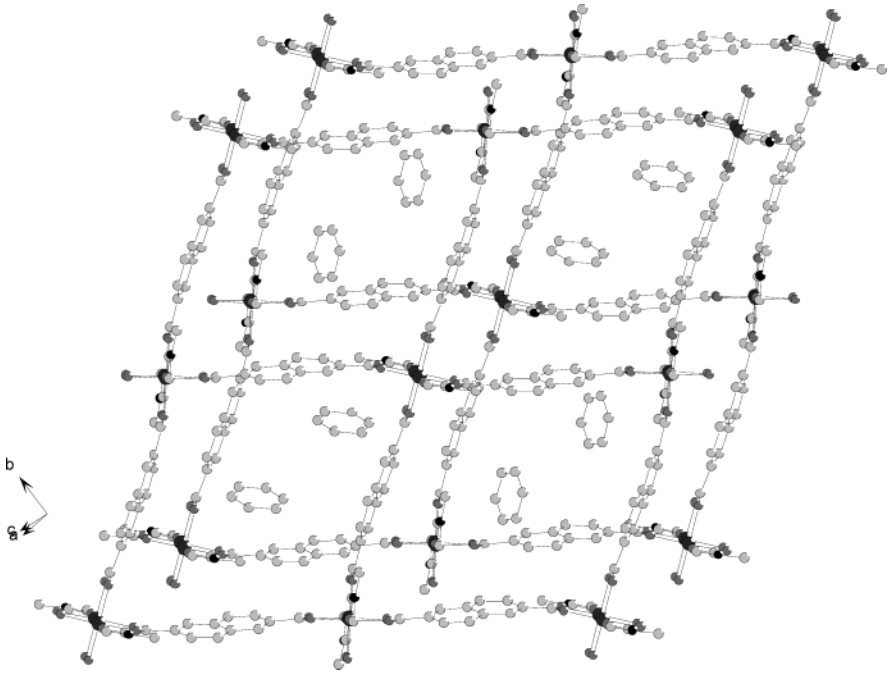

Figure 3. View, in projection, of a two layer sequence of the zinc 2,6-naphthalene dicarboxylate MOF-105 structure showing that each layer is offset with respect to the next. The DMF ligands bound to the zinc atoms project up and down into the available space. Solvent molecules are not shown, and hydrogen atoms are omitted for clarity. Light gray represents C; black represents N; large, dark gray represents Zn; small, dark gray represents O.

using a sequence of saturation recovery followed by quadrupole echo. Time between saturation pulses was 400 μs, and the number of saturation pulses was 100 for each experiment. The delay between pulses was 2.00 μs. T_1 values were calculated from the peak integrals and fitted to the Arrhenius equation to calculate the activation energy, E_a.

Selective Uptake of Xylene Isomers. To investigate the selective uptake of xylene isomers upon crystallization, small quantities of the title compound were prepared in the presence of 1:1 mixtures of *p*- and *o*- or *m*-xylene in the parent solution. Mixtures of (i) *p*-xylene (C_8H_{10}) and perdeuterated *o*-xylene (C_8D_{10}) and (ii) *p*-xylene (C_8H_{10}) and perdeuterated *m*-xylene (C_8D_{10}) were used. The resulting crystals were analyzed by TG-MS (A Netszch Jupiter thermogravimetric analyzer coupled with a Balzer MID mass spectrometer) by examination of the mass numbers corresponding to the parent ions of perdeuterated and nondeuterated xylenes (116 and 106 *m*/*z*), as well as fragment ions formed by demethylation (e.g., 98 and 91 *m*/*z* for the two compounds, respectively).

To quantify the selectivity of the inclusion, a larger batch of the zinc naphthalene dicarboxylate was crystallized from a mixture of *p*- and *o*-xylene. The sample was transferred to a vacuum line, evacuated, and heated to a temperature at which the xylenes (and dimethylformamide) are known (from the results of thermogravimetric analysis) to be removed from the material. The liberated products were collected in a coldfinger,

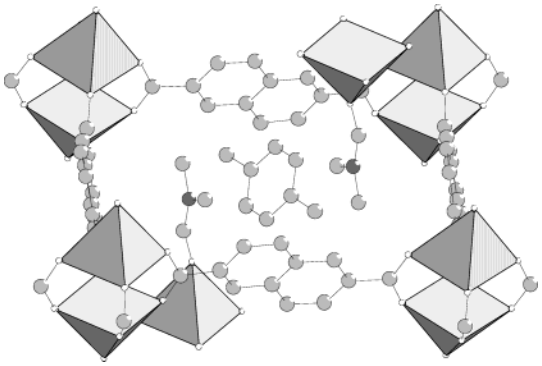

Figure 4. View of the *p*-xylene molecule included within the cavities of compound **4**. The *p*-xylene is in the space defined within the zinc 2,6-naphthalene dicarboxylate layer and further constrained by DMF ligand molecules extending from layers above and below. ZnO_5 units are represented as coordination polyhedra. Hydrogen atoms are omitted for clarity.

dissolved in dichloromethane, and analyzed on a gas chromatograph fitted with a packed column with a stationary phase of 10% APL on Chromasorb WAW that had been calibrated for xylenes.

III. Theoretical Methodology

Density functional theory-based calculations were performed using CASTEP (version 4.2)[17] implemented on an IBM/RS6000 parallel machine with three nodes, each with four 375 MHz power3 processors. Exchange and correlation energies were treated using the generalized gradient approximation (GGA) based on the Perdew and Wang exchange and correlation functional (PW91). The Perdew and Wang functional has recently been shown to give the best representation of interaction energies in systems where dispersion forces are significant.[18] Ultrasoft pseudopotentials were used with a kinetic energy cutoff of 340 eV for the planewave basis set with a finite basis correction being applied during unit cell optimizations. The atomic positions of both the lattice and the occluded molecules (when included) were allowed to move during the optimizations.

IV. Experimental Results and Discussion

Synthesis. Four crystalline solids were prepared and characterized by crystallization in the presence of DMF only as a solvent, **1**, of DMF and benzene, **2**, of DMF and toluene, **3**, and of DMF and *p*-xylene, **4**. The solids were characterized by elemental analysis, TG-MS, and ^{13}C MAS NMR to confirm the presence of the included molecules.

*$[Zn_2(ndc)_2(DMF)_2]\cdot 1.6DMF$ (**1**).* ^{13}C NMR (125 MHz, 25 °C, 7.3 kHz): $\delta = 35.7$ and 30.9 ($\mathbf{C}H_3)_2NCHO$; 172.1 $(CH_3)_2N\mathbf{C}HO$; 128.5−134.4 ndc aromatic; 178.0 ndc carbonyl.

*$[Zn_2(ndc)_2(DMF)_2]\cdot C_6H_6$ (**2**).* Elemental analysis: measured 53.72% C, 4.25% H, 3.83% N; calculated 55.2% C, 4.08% H, 3.57% N. ^{13}C NMR (125 MHz, 25 °C, 8.7 kHz): $\delta = 34.2$ and 30.3 ($\mathbf{C}H_3)_2NCHO$; 167.5 $(CH_3)_2N\mathbf{C}HO$; 128.1−136.0 ndc aromatic; 171.5 ndc carbonyl.

*$[Zn_2(ndc)_2(DMF)_2]\cdot C_7H_8$ (**3**).* Elemental analysis: measured 54.94% C, 4.41% H, 3.66% N; calculated 55.60% C, 4.26% H, 3.51% N. ^{13}C NMR (125 MHz, 25 °C, 8.7 kHz): $\delta = 34.3$ and 30.9 ($\mathbf{C}H_3)_2NCHO$; 167.4 $(CH_3)_2N\mathbf{C}HO$; 128.5−135.0 ndc and toluene aromatic; 172.1 ndc carbonyl; 20.4 $\mathbf{C}H_3C_6H_5$.

*$[Zn_2(ndc)_2(DMF)_2]\cdot C_8H_{10}$ (**4**).* Elemental analysis: measured 53.71% C; 4.19% H, 2.97% N; calculated 56.2% C, 4.4% H, 3.45% N. ^{13}C NMR (125 MHz, 25 °C, 10.0 kHz): $\delta = 34.2$ and 31.0 ($\mathbf{C}H_3)_2NCHO$; 167.5 $(CH_3)_2N\mathbf{C}HO$; 128.1−134.4 ndc and xylene aromatic; 171.5 ndc carbonyl; 19.2 $(\mathbf{C}H_3)_2C_6H_4$.

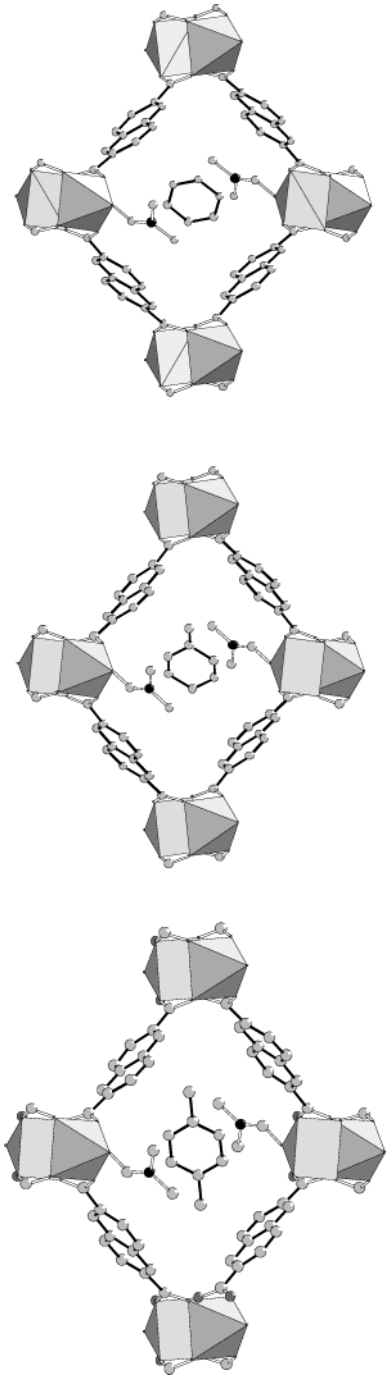

Figure 5. Views down the *a* axis of the molecules benzene, toluene, and *p*-xylene within the "channels" of compounds **2**, **3**, and **4**. Only one of the two possible orientations of toluene is represented. Hydrogen atoms are omitted for clarity.

TABLE 2: Unit Cell Parameters of Compounds 1, 2, 3, and 4 Showing the Trends According to the Guest Solvent Molecules[a]

compound no., included solvent	*a* (Å)	*b* (Å)	*c* (Å)	*β* (deg)
1, DMF	8.075(1)	16.891(2)	12.673(2)	92.90(1)
2, benzene	8.3404(2)	15.6598(43)	13.0079(35)	91.340(5)
3, toluene	8.2076(2)	16.4630(1)	12.9685(4)	93.141(2)
4, *p*-xylene	7.9731(16)	16.9462(33)	12.9218(25)	92.798(4)

[a] Data on compound **1** were obtained from powder diffraction data using the le Bail refinement option within the GSAS suite of programs.[19]

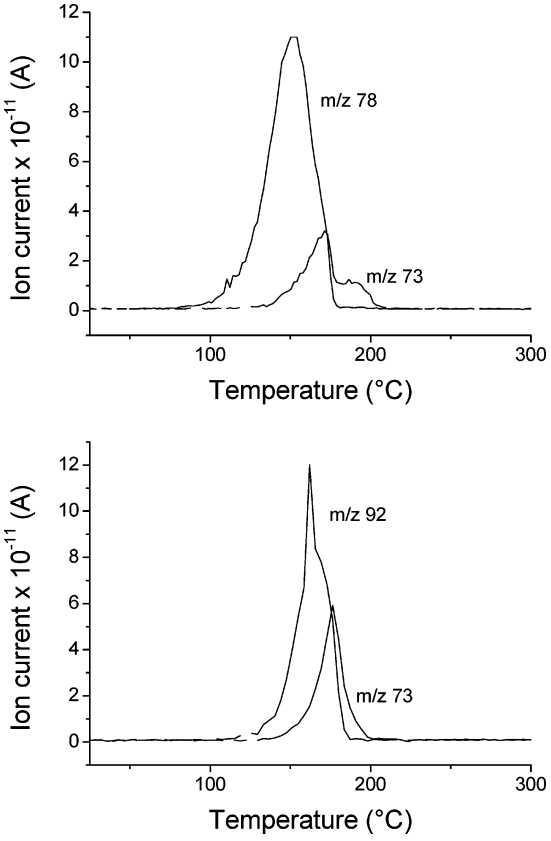

Figure 6. TG-MS plots showing the rate of loss of included molecules occurring before the loss of structural DMF ligands for (above) benzene lost from **2** and (below) toluene lost from **3**.

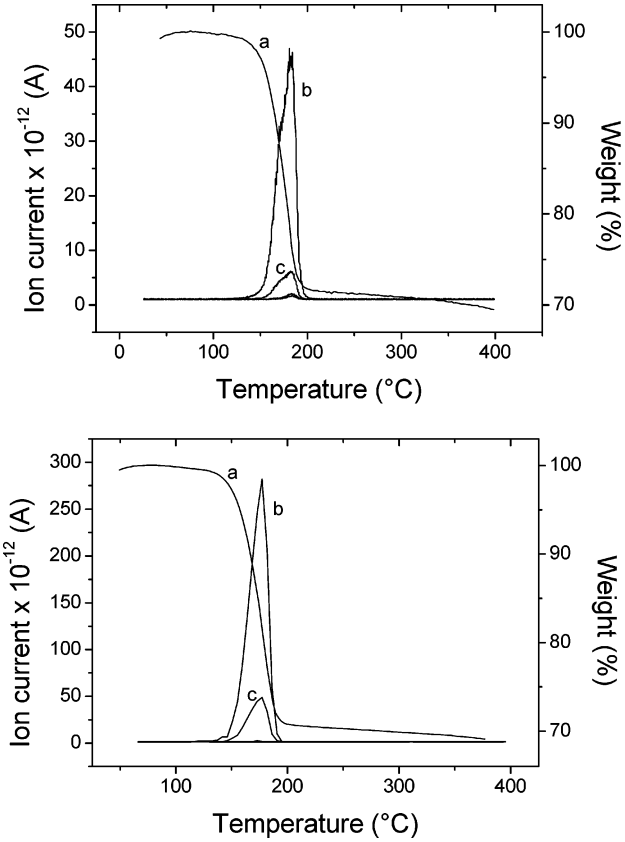

Figure 7. Thermogravimetric analyses (a) and mass spectrometric analyses of compounds prepared by crystallization from solvent mixtures containing equimolar quantities of (above) perdeuterated *m*-xylene (C_8D_{10}) and *p*-xylene (C_8H_{10}) and (below) perdeuterated *o*-xylene (C_8D_{10}) and *p*-xylene (C_8H_{10}). These show the substantial presence of the molecular ion and main fragments from *p*-xylene, *m*/*z* 106 (c) and *m*/*z* 91 (b), whereas corresponding peaks from perdeuterated *m*- and *o*-xylenes (*m*/*z* 116 and 98) are very small.

The results of the single-crystal analyses on these phases are described in Table 1 and the X-ray powder diffraction patterns of the crystalline products are shown in Figure 1. The powder data confirm that the single-crystal structures are representative of the bulk, and the bulk analyses of **2**, **3**, and **4** confirm this. Compound **1** loses DMF on standing and was very difficult to analyze unambiguously. The composition was estimated from the TGA analysis. Attempts to synthesize the zinc 2,6-naphthalene dicarboxylates in the presence of mixtures of DMF and *o*- or *m*-xylene resulted in poorly crystalline phases and TG-MS measurements showed that these materials do not contain the aromatic additives.

The main crystalline phases are found by single-crystal diffraction experiments to possess the same basic framework structure, and these single-crystal structures were shown by simulation of the powder patterns to be representative of the bulk crystalline phases. However, single crystals of compound **1**, prepared in the absence of aromatic hydrocarbons, were found to be highly unstable, and good quality data could not be obtained by single-crystal diffraction studies. The main difference between the crystalline structures is that the molecules included in cavities within the structure are different, and these are accommodated in the structure by different distortions of the framework.

The zinc 2,6-naphthalene dicarboxylate (ndc)/DMF framework structure ($Zn(O_2C-C_{10}H_8-CO_2)\cdot O(H)CN(CH_3)_2$) is made up of a stacked arrangement of layers of zinc ndc.[8] Within each layer, units of two square pyramidally coordinated zinc coordination polyhedra are linked by bidentate carboxylate groups, the fifth coordinating oxygen on each zinc coming from the oxygen of the DMF ligands that point up and down from these layers (Figure 2). Each layer therefore possesses an array of edge-sharing rings, individually made up of four $(ZnO_5)_2$ units and four naphthalene dicarboxylate units, with the plane of the naphthalene groups running approximately normal to the layer. Each ring therefore encloses a rhombus of apparently free space with diagonal dimensions of 21 and 15 Å. The layers stack on one another along the [101] direction with DMF molecules coordinated apically to the zinc atoms being directed into the intralayer spaces above and below (Figure 3). One DMF molecule projects into any one ring from the layer above and one from the layer below, partly filling the free space but leaving a cavity between the DMF molecules into which occluded molecules can fit. This is illustrated for the inclusion compound with *para*-xylene in Figure 4. The structure can accommodate molecules of different shapes, for example, DMF, benzene, toluene, and *p*-xylene. The positions of the different aromatic hydrocarbons within channels in the structure, viewed down *a*, are given in Figure 5. The crystal diffraction studies identify the location of these molecules within the cavity and the way in which the unit cell changes as different molecules are included. Table 2 (which includes the results of X-ray powder diffraction of **1**) reveals that the largest changes in unit cell dimensions are in the unit cell vectors *a* and *b*. On going from the structure with included benzene to that with included *p*-xylene, for example, the *a* axis decreases by 4.4% whereas the *b* axis increases by 8.2%. The experimental data indicate that the structure does not form in the presence of *o*- or *m*-xylene or mesitylene when crystallizing under these conditions. Toluene

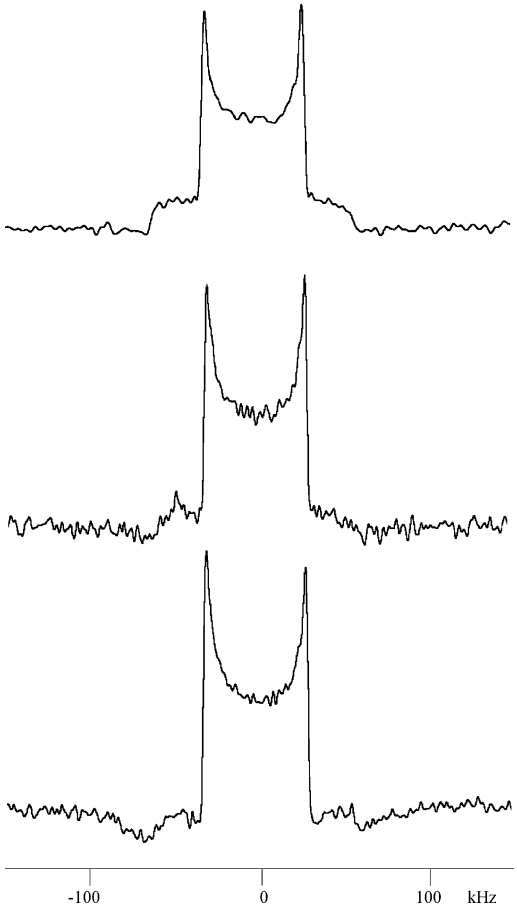

Figure 8. Variable temperature ^{2}H NMR of compound **2**, prepared with perdeuterated benzene, C_6D_6, collected at 294 (top), 193 (middle), and 148 K (bottom).

is included into the centrosymmetric structure with static disorder.

Behavior of the Solids upon Heating. Thermogravimetric analyses of the crystalline solids reveal differences in behavior according to the molecules that are included. For solids containing benzene, toluene, and *p*-xylene, two distinct weight loss events are observed. The first (at around 150 °C) is shown by TG-MS analysis to result from loss of DMF and benzene, toluene, or *p*-xylene, and this is consistent with the mass loss. The framework starts to lose CO_2 at 450 °C and completely collapses around 500 °C. For the sample **1** containing only DMF, kept in the presence of DMF vapor to prevent transformation, there are four distinct weight loss events; a steep weight loss from 30 to 80 °C from free solvent, well-defined weight loss steps at ca. 120 and 200 °C corresponding to structural DMF, and a steep weight loss at 475 °C corresponding to loss of CO_2. The third peak can be attributed to the loss of DMF liganded to zinc, whereas the second peak is due to loss of included DMF corresponding to ca. 1.6 molecules per cavity site.

TG-MS reveals that loss of benzene from **2** begins at slightly lower temperatures than loss of toluene from the toluene-containing analogue (Figure 6)—below 100 °C. This indicates the relative ease with which benzene can be liberated from the framework when compared to the larger toluene. X-ray powder diffraction of samples heated to remove the DMF and the included molecules shows that they lose crystallinity. Interestingly, if the sample containing benzene is left in the air at 60 °C overnight, there is a structural transformation to a crystalline phase, but this does not possess the layered arrangement of the parent material (the X-ray powder profile is not similar).

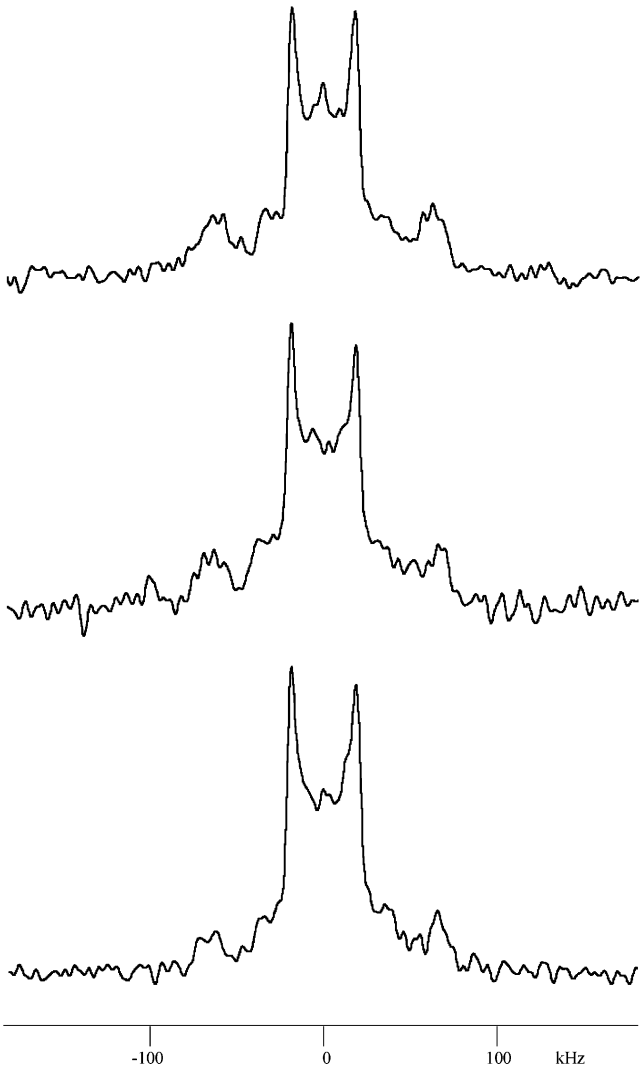

Figure 9. Variable temperature ^{2}H NMR of compound **3**, prepared with perdeuterated toluene, C_7D_8, collected at 294 (top), 233 (middle) and 193 K (bottom).

Selective Inclusion of *p*-Xylene during Crystallization. The crystallization and TGA/TG-MS experiments indicate that the framework that we discuss here is stabilized (to thermal decomposition) by the inclusion of the aromatics benzene, toluene, and *p*-xylene and that the presence of *o*- and *m*-xylene inhibit the crystallization. We were therefore interested to see whether crystallization from solution would result in selective uptake of the p-isomer from a mixture of xylenes. Experiments performed by crystallizations in the presence of mixtures of deuterated *o*- or *m*-xylene and nondeuterated *p*-xylene isomers, as previously described, indicated that the p-isomer is taken up preferentially. TG-MS of samples crystallized from mixtures of C_8H_{10} *p*-xylene and C_8D_{10} *o*-xylene or C_8D_{10} *m*-xylene are given in Figure 7, showing that only traces of *o*- or *m*-xylene are present. Quantitative analysis by gas chromatography of the xylenes included from a 1:1 addition of *o*- and *p*-xylene to the crystallizing mix indicated that the included mixture is made up of 98% of the p-isomer.

Mobility of the Guest Molecules. The materials may therefore be considered as frameworks into which aromatic hydrocarbons are selectively included upon crystallization. To examine the mobility of the guest molecules within cavities in the structure, ^{2}H static NMR was performed on samples crystallized in the presence of perdeuterated benzene and

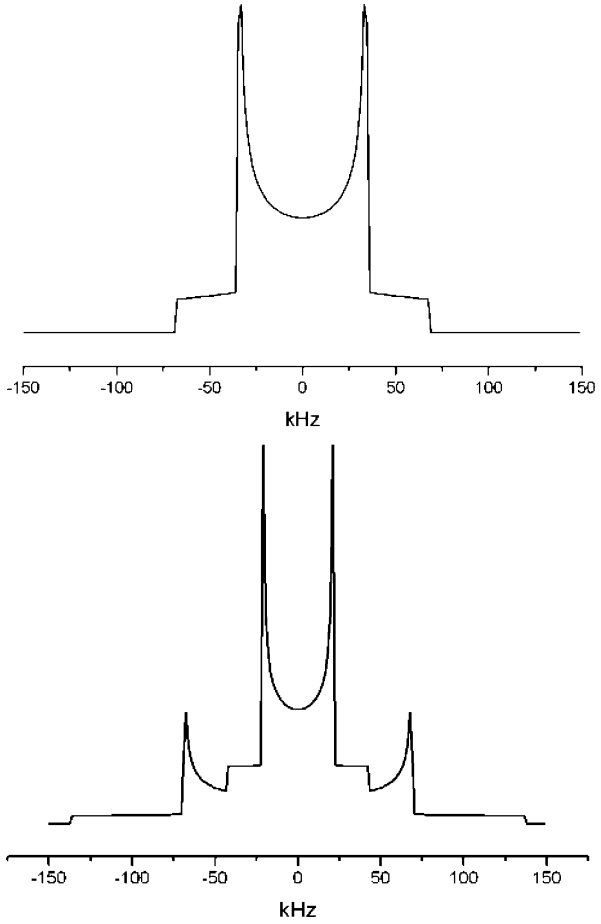

Figure 10. Simulated ^{2}H NMR spectra for in-plane rotation of C_6D_6 molecules about the 6-fold axis (above) and for a static aromatic ring and fast hopping $-CD_3$ group about its 3-fold axis in C_7D_8 toluene (below).

toluene. ^{2}H NMR of compound **2** displays a Pake pattern with a double horn splitting of 68 kHz (Figure 8) indicating an in-plane rotation of benzene molecules about the 6-fold axis. Simulations reveal that the line shapes do not differentiate between alternate models of hopping of C−D bonds from one site to another (Figure 9) and benzene molecules spinning about the 6-fold axis. However, X-ray diffraction data, which indicates the time-averaged location of the benzene in the cavity, indicates that motion of the former type is occurring. Variable temperature studies show that the motion is not arrested at a temperature as low as 123 K. T_1 relaxation time measurements over the temperature range indicate an activation energy of rotation of 6 ± 1 kJ mol^{-1}. For compound **3**, two Pake doublets (Figure 10) were observed indicating that the aromatic ring is static (double horn splitting of 137 kHz) while the $-CD_3$ groups are hopping rapidly around the Ph$-CD_3$ bond (double horn splitting of 42 kHz), which is not frozen even at 173 K. This is in accordance with the simulated spectrum for this motion (Figure 9).

These observations are consistent with the structural studies and indicate the constrained motion of the solvent molecules. The only possible mode of motion for benzene seems to be the rotation about the 6-fold axis, but the bulky CD_3 group prevents such a mode for toluene.

V. Computational Results and Discussion

The ability of the computational DFT approach to model these compounds accurately was assessed by performing calculations

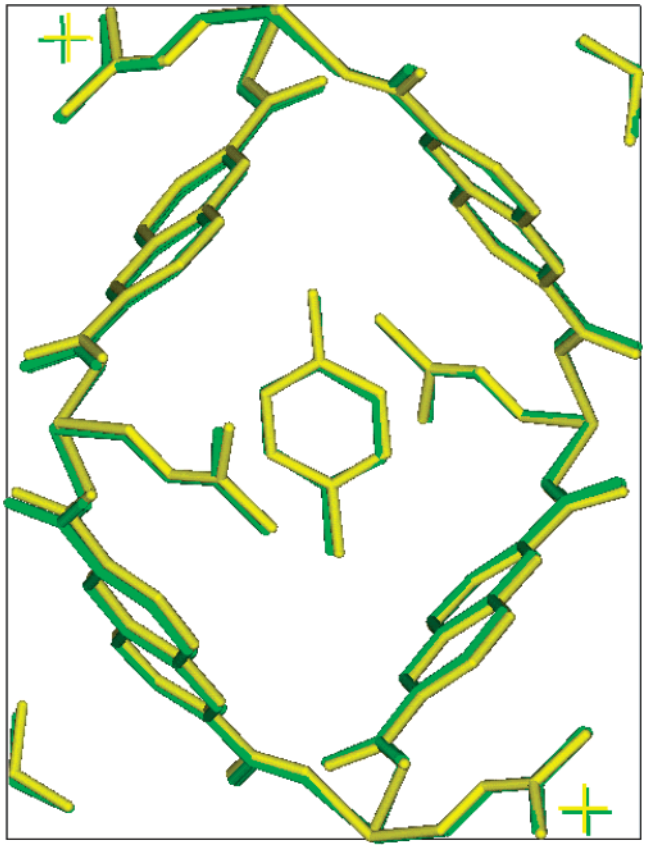

Figure 11. Overlaid structures obtained experimentally from single-crystal diffraction (yellow) and simulated using density functional calculations at constant volume for *p*-xylene in compound **4** (green).

at both constant volume and constant pressure. Periodic boundary conditions were applied to the structures obtained from experiment and the positions of the atoms (and in the case of the constant pressure calculations, the unit cell parameters) were allowed to vary until a minimum energy configuration was obtained. For the compound including toluene, the two toluene molecules in the unit cell were allowed to "order" as demanded by the crystallographic symmetry. Figure 11 shows the close agreement obtained between the DFT-optimized coordinates at constant volume and the experimental coordinates for the structure with included *p*-xylene. Similar agreement was obtained for the toluene- and benzene-containing solids.

Results from the constant pressure calculations also show good agreement with the experimental results, Table 3. The optimized unit cell parameters follow the trends observed from the XRD experiments.

DFT calculations were also performed on the hypothetical case of *m*-xylene within the zinc 2,6-naphthalene dicarboxylate framework to understand better the nature of the inclusion process. If we assume that one of the $-CH_3$ groups in *m*-xylene will position itself in the same location as the $-CH_3$ groups in *p*-xylene, then there are two chemically nonequivalent ways for the *m*-xylene to be included within the MOF-105 structure, Figure 12. The two orientations vary mainly in the proximity of the second methyl group to the DMF molecule from the adjacent layer. Calculations were performed for both *m*-xylene molecules with the methyl groups close to the DMF ligand, for both directed away from the DMF ligand, and for one molecule in each environment.

From Table 3, it can be seen that *p*-xylene and toluene have the highest binding energies, followed by benzene and *m*-xylene. The trends obtained for the binding energies of benzene, toluene,

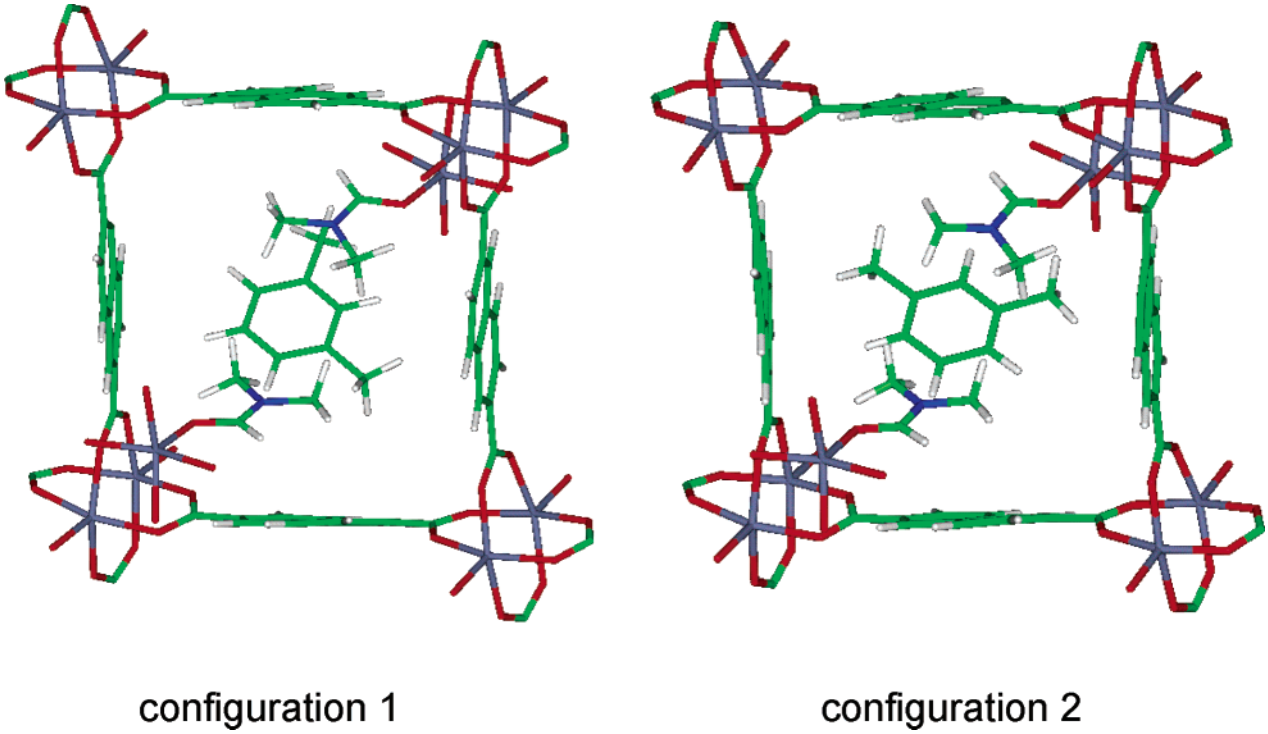

Figure 12. Simulated energy-minimized positions of *m*-xylene in the two hypothetical chemically distinct configurations available in the MOF-105 structure: (left) configuration 1; (right) configuration 2.

TABLE 3: Unit Cell Constants of the Zinc 2,6-Naphthalene Dicarboxylate as a Function of the Included Molecule Determined Experimentally by Single-Crystal Diffraction and Simulated by Density Functional Theory Calculations at Constant Pressure and the Calculated Binding Energy per Included Molecule

included compound	exptl cell constants ($P2_1/c$) *a*, *b*, *c* (Å), β (deg)	simulated cell constants ($P2_1/c$) *a*, *b*, *c* (Å), β (deg)	binding energy (eV/molecule)
benzene	8.34, 15.65, 13.01, 92.88	8.43, 15.88, 13.14, 92.46	−0.24
toluene	8.21, 16.46, 12.97, 93.14	8.32, 16.64, 13.15, 94.26	−0.33
p-xylene	7.97, 16.94, 12.92, 92.80	8.13, 17.08, 12.99, 94.16	−0.46
m-xylene (config. 1)	not formed	8.12, 17.30, 13.24, 95.84	−0.24
m-xylene (config. 2)	not formed	8.18, 17.21, 13.16, 95.61	−0.24
m-xylene (configs. 1 and 2)	not formed	8.02, 17.11, 12.97, 94.22	−0.11

and *p*-xylene are in agreement with the observations from the TGA experiments, which indicate that benzene is lost more readily than toluene. The hypothetical *meta*-xylene case is interesting, since the ordered configurations 1 and 2 appear to be able to arrange the structure to one with an energy similar to that of benzene but less favorable than that of the *p*-xylene. Where *m*-xylene molecules with different orientations with respect to the DMF of the framework are present in the unit cell, however, it is notable that the *a* axis is considerably shorter and the structure less stable (*m*-xylene binding energy of only 0.11 eV per molecule). It may be that under the conditions of synthesis the completely ordered arrangements of either configuration 1 or configuration 2 cannot form and that this contributes to the inability of the solid to form in the presence of *m*-xylene.

At the synthesis temperature, the $-CH_3$ group at the meta position in *meta*-xylene, which is in close proximity to a DMF group in the host lattice, will be freely rotating. The effect of this on the binding energy has been estimated by taking the energy-minimized configuration for this meta isomer, rotating the $-CH_3$ group through 60°, and then holding the molecule fixed at this conformation while allowing the lattice framework to relax fully. This results in an observed further reduction of the binding energy by 0.12 eV for configuration 1 and by 0.07 eV for configuration 2.

Furthermore, it would seem likely that the solids can grow via a layer mechanism. By removing the DMF group from above the organic molecule, an estimate of the binding energy to the growing surface (neutral in charge) has been obtained for *m*-xylene (configurations 1 and 2) and for *p*-xylene. For *p*-xylene, the binding energy per molecule is −0.482 eV, whereas for the *m*-xylene the binding energies are −0.143 eV (configuration 1) and −0.188 eV (configuration 2). *p*-Xylene is much more strongly bound to the growing surface than *m*-xylene in either of the two configurations, and this may be responsible for the selective uptake of the para isomer.

In summary, the DFT calculations reproduce these complex guest−host structures in excellent agreement with those determined experimentally. The key reason for the significant difference in the calculated binding energies for *p*- and *m*-xylene can be attributed to the expansion of the unit cell in the *b*-direction necessary to accommodate the meta isomer. This expansion leads to a more strained lattice, resulting in a reduction in the observed binding energy. The expansion of the lattice necessary to accommodate *m*-xylene at the experimental synthesis temperature will be greater than those observed in the theoretical calculations, which are effectively performed at 0 K. It is interesting to note that the close proximity of the CH_3 group at the meta position to one of the DMF units seems to be a much less significant factor in the reduced binding energy

observed than the expansion of the unit cell necessary to accommodate the molecule. The calculations undertaken to simulate binding to the surface of the structure with no DMF sited immediately above the xylene isomers are of similar magnitude to those obtained when the isomers are fully occluded. Furthermore, allowing the $-CH_3$ group at the meta position to rotate lowers the observed binding energy. Although all of these factors may contribute to the inability of the solid to form in the presence of *m*-xylene, the expansion of the unit cell and the consequent strain that it induces in the host lattice appears to be the most significant factor.

VI. Conclusions

The zinc 2,6-naphthalene host framework (previously shown to form in the presence of chlorobenzene as MOF-105) has been crystallized from DMF solution in the absence and presence of the aromatic hydrocarbons benzene, toluene, and *p*-xylene. The crystallizing solid takes up *p*-xylene with high selectivity from mixtures with *o*- or *m*-xylene, and indeed, the structure does not crystallize in the presence of *o*- or *m*-xylene or mesitylene. The framework is made up of layers that possess cavities, partially filled from above and below by DMF molecules coordinated to zinc atoms from adjacent layers. The aromatic molecules are included in these cavities in the flexible framework, the unit cell parameters of which vary by up to 8%. The inclusion of aromatics stabilizes the framework thermally with respect to the solid that only contains DMF. The larger toluene and xylene are retained more strongly in the structure than benzene, but heating to 150 °C and above results in loss of the aromatic hydrocarbons and the DMF ligands for all solids.

A combination of X-ray diffraction and variable temperature ^2H NMR gives detailed information on the location and mobility of the included molecules. Benzene is found to be held within the cavity but to be jumping rapidly about its 6-fold axis, even at low temperatures. Toluene, by contrast, is held rigidly in place, the only motion being the rapid motion of methyl groups. Included *p*-xylene would be expected to show similar motion to toluene.

Computational simulation via energy minimization at constant volume and constant pressure using the density functional theory calculations using the CASTEP program are shown to reproduce accurately the experimentally determined structures. Furthermore, they shed light on the selectivity of the crystallizing structure for the uptake of *p*-xylene compared to other xylene isomers. The *m*-xylene could only be accommodated in the growing structure by a significant distortion of the framework, which leads to a significant energy penalty. In addition, because *m*-xylene molecules have a lower symmetry than *p*-xylene, they could be included in two chemically distinct orientations, and a combination of these two would result in a further rise in the structure's energy.

In summary, the zinc 2,6-naphthalene dicarboxylate framework acts as a flexible inclusion host that takes up aromatic hydrocarbons during crystallization. For xylenes, this uptake may be highly selective. The physical properties of these solids are readily studied by crystallography and NMR and simulated by density functional theoretical calculations. Further experimental and theoretical studies of related materials in selective adsorption are in progress.

Acknowledgment. We gratefully acknowledge the EPSRC for financial support.

References and Notes

(1) (a) Kim, J.; Chen, B.; Reineke, T.; Li, H.; Eddaoudi, M.; Moler, D. B.; O'Keeffe, M.; Yaghi, O. M. *J. Am. Chem. Soc.* **2001**, *123*, 8239. (b) Eddaoudi, M.; Moler, D. B.; Li, H.; Chen, B.; Reineke, T. M.; O'Keeffe, M.; Yaghi, O. M. *Acc. Chem. Res.* **2001**, *34*, 319.

(2) (a) Li, H.; Davis, C. E.; Groy, T. L.; Kelley, D. G.; Yaghi, O. M. *J. Am. Chem. Soc.* **1998**, *120*, 2186. (b) Li, H.; Eddaoudi, M.; Groy, T. L.; Yaghi, O. M. *J. Am. Chem. Soc.* **1998**, *120*, 8571.

(3) Li, H.; Eddaoudi, M.; O'Keeffe, M.; Yaghi, O. M. *Nature* **1999**, *402*, 276.

(4) (a) Vodak, D. T.; Braun, M. E.; Kim, J.; Eddaoudi, M.; Yaghi, O. M. *Chem. Commun.* **2001**, 2534. (b) Rosi, N. L.; Eddaoudi, M.; Kim, J.; O'Keeffe, M.; Yaghi, O. M. *Angew. Chem., Int. Ed.* **2002**, *41*, 284.

(5) (a) Eddaoudi, M.; Kim, J.; Rosi, N.; Vodak, D.; Wachter, J.; O'Keeffe, M.; Yaghi, O. M. *Science* **2002**, *295*, 469. (b) Rosi, N. L.; Eckert, J.; Eddaoudi, M.; Vodak, D. T.; Kim, J.; O'Keeffe, M.; Yaghi, O. M. *Science* **2003**, *300*, 1127.

(6) Edgar, M.; Mitchell, R.; Slawin, A. M. Z.; Lightfoot, P.; Wright, P. A. *Chem.—Eur. J.* **2001**, *7*, 5168.

(7) Zhu, L.-N.; Zhang, L. Z.; Wang, W.-Z.; Liao, D.-Z.; Cheng, P.; Jiang, Z.-H.; Yan, S.-P. *Inorg. Chem. Commun.* **2002**, *5*, 1017.

(8) Eddaoudi, M.; Kim, J.; Vodak, D.; Sudik, A.; Wachter, J.; O'Keeffe, M.; Yaghi, O. M. *Proc. Natl. Acad. Sci. U.S.A.* **2002**, *99*, 4900.

(9) Spiess H. W, *Adv. Polym. Sci.* **1985**, *66*, 22.

(10) Bull, L. M.; Henson, N. J.; Cheetham, A. K.; Newsam, J. M.; Heyes, S. J. *J. Phys. Chem.* **1993**, *97*, 11776.

(11) Goncalves, J. A. S.; Portsmouth, R. L.; Alexander, P.; Gladden, L. F. *J. Phys. Chem.* **1995**, *99*, 3317.

(12) Auerbach, S. M.; Bull, L. M.; Henson, N. J.; Metiu, H. I.; Cheetham, A. K. *J. Phys. Chem.* **1996**, *100*, 5923.

(13) Sato, T.; Kunimori, K.; Hayashi, S. *Phys. Chem. Chem. Phys.* **1999**, *1*, 3839.

(14) Kohn, W.; Sham, L. J. *Phys Rev. A* **1965**, *140*, 1133.

(15) Sheldrick, G. M. *SHELXTL, Program for the solution of crystal structures*; University of Göttingen: Göttingen, Germany, 1993.

(16) Macho, V.; Brombacker, L.; Spiess, H. W. The NMR−WEBLAB: an Internet Approach to NMR Line shape Analysis. *Appl. Magn. Reson.* **2001**, *20*, 405.

(17) Payne, M. C.; Teter, M. P.; Allan, D. C.; Arias, T. A.; Joannopoulos, J. D. *Rev. Mod. Phys.* **1992**, *64*, 1045.

(18) Tsuzuki, S.; Luthi, H. P. *J. Chem. Phys.* **2001**, *14*, 3949.

(19) Larson, A.; Von Dreele, R. *Generalized Crystal Structure Analysis System*; Los Alamos National Laboratory: Los Alamos, NM, 1988.